Provided for non-commercial research and education use.
Not for reproduction, distribution or commercial use.

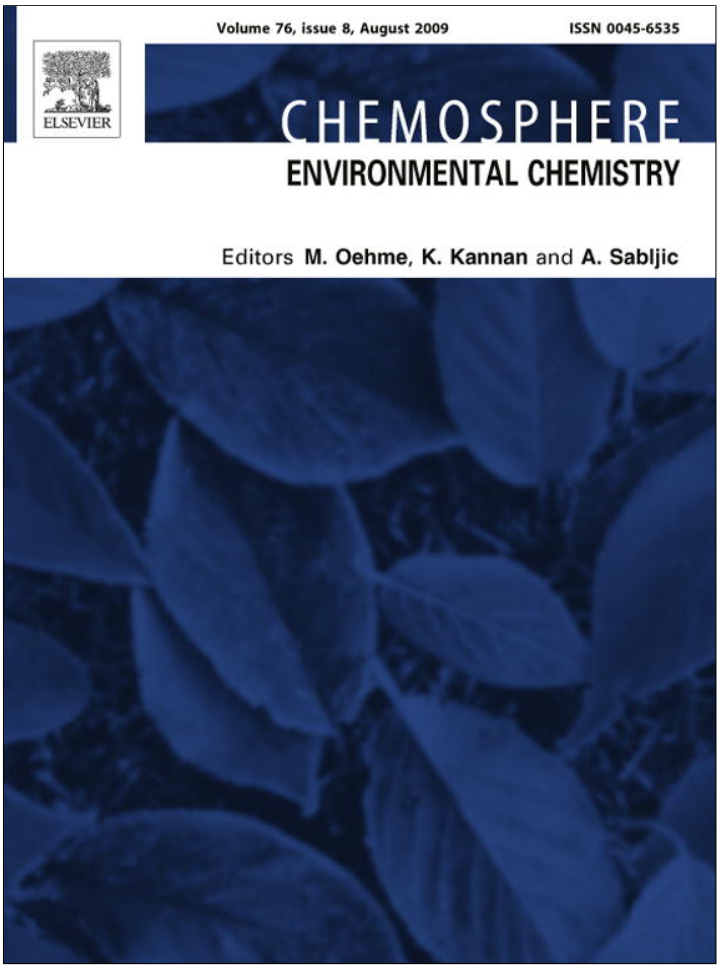

This article appeared in a journal published by Elsevier. The attached copy is furnished to the author for internal non-commercial research and education use, including for instruction at the authors institution and sharing with colleagues.

Other uses, including reproduction and distribution, or selling or licensing copies, or posting to personal, institutional or third party websites are prohibited.

In most cases authors are permitted to post their version of the article (e.g. in Word or Tex form) to their personal website or institutional repository. Authors requiring further information regarding Elsevier's archiving and manuscript policies are encouraged to visit:

http://www.elsevier.com/copyright

Author's personal copy

Chemosphere 76 (2009) 1023–1027

Contents lists available at ScienceDirect

Chemosphere

journal homepage: www.elsevier.com/locate/chemosphere

A fluorescence quenching study of the interaction of Suwannee River fulvic acid with iron oxide nanoparticles

Adriana Manciulea, Andy Baker *, Jamie R. Lead

School of Geography, Earth and Environmental Sciences, University of Birmingham, Edgbaston, Birmingham B15 2TT, United Kingdom

ARTICLE INFO

Article history:
Received 20 January 2009
Received in revised form 28 April 2009
Accepted 29 April 2009
Available online 27 May 2009

Keywords:
Fluorescence
Dissolved organic matter
Stern–Volmer
Nanoparticle

ABSTRACT

The fluorescence quenching behaviour of a manufactured nanoparticle (NP, iron oxide, 7 nm) on the standard Suwannee River fulvic acid (SRFA) was investigated for the first time. Size, aggregation and fluorescence was examined as a function of NP:SRFA ratio and of pH. Aggregation state varied as both a function of pH and NP:SRFA ratio, with maximum aggregation at near neutral pH values (6–8). SRFA fluorescence quenching increased non-linearly with increasing NP concentrations (>0.22 $\times$ 10^{-3} M iron nanoparticles), indicating the complex nature of NP:SRFA interactions. Aggregates of iron oxide present at pH 7–8 appeared to have a much larger effect on quenching compared with dispersed NPs or dissolved phase iron. Fluorescence quenching is demonstrated to indicate different mechanisms of NP:SRFA binding with pH.

© 2009 Elsevier Ltd. All rights reserved.

1. Introduction

Nanotechnology may be defined as the production and use of nanoscale material, with the nanoscale defined as between 1 and 100 nm and nanoscience deals with the scientific properties of materials in this range. The recent development of nanotechnology into a major industry has raised concerns over the possible fate, behaviour and ecotoxicology of manufactured nanoparticles (NPs), and our knowledge is severely limited in this area (Lead and Wilkinson, 2006; Nowack and Bucheli, 2007). The small sizes (and related parameters such as increased specific surface area, SSA) give NPs properties which are quantitatively and qualitatively different from the larger scale particles, even where there is no difference in chemical properties (Madden and Hochella, 2005; Madden et al., 2006). These changes are related to their specific surface area (SSA), surface energy, size quantum constraint and other factors. Despite their abundant applications in the industrial (Paradise and Goswami, 2007), commercial and biomedical (Lacerda et al., 2006) fields, studies have shown that they are potentially toxic to humans (Soto et al., 2005; Tian et al., 2006; Casey et al., 2007), mammalian organisms (Bermudez et al., 2004; Oyewumi et al., 2004; Jia et al., 2005; Muller et al., 2006), fish (Oberdorster, 2004; Smith et al., 2007) and bacteria (Fortner et al., 2005; Brayner et al., 2006; Lyon et al., 2006; Fabregas et al., in press; Hu et al., 2009). Knowledge of the environmental fate and behaviour of NPs is poor, although a few laboratory based studies exist (Wiesner et al., 2006; Giasuddin et al., 2007; Seeger et al., 2009).

Iron oxide nanoparticles are an important type of NP, based on production volume and are also relevant in aquatic systems as they are representative of the shell of core–shell zerovalent iron NPs used in contaminated land remediation (Zhang, 2003) and which are highly likely to be discharged into the aquatic environment (Soto et al., 2005) due to their increasing use in applications for removal of contaminants from the environment (Ponder et al., 2001; Zhang, 2003; Nurmi et al., 2005; Giasuddin et al., 2007; Phenrat et al., 2007). Iron oxides are also an important component of colloids in aquatic and terrestrial systems and use of model iron oxide NPs may allow further understanding of these natural materials.

The use of synthesised iron oxides and their interaction with natural organic macromolecules (NOM) such as humic substances (HS) thus gives us potential insight into both the natural system where iron oxide and NOM are key colloidal carriers of pollutants (Lyven et al., 2003), and also on likely behaviour of manufactured NPs. It is currently of great importance to study how NOM can interact with NPs and influence their fate and behaviour through alteration in, for instance, dispersion state (Hyung et al., 2007).

Humic substances (HS) form a major component of NOM (Aiken et al., 1985; Chen et al., 2003). They play a vital role in the environment by influencing transport processes and bioavailability of nutrients and contaminants (pollutants) (Buffle, 2006; Lead and Wilkinson, 2006) and may have a similar impact on NP fate and behaviour in the environment. Recent reports have shown interactions between HS and gold nanoparticles (Diegoli et al., 2008), zerovalent iron (Giasuddin et al., 2007), fullerenes (Chen and Elimelech, 2007), iron oxide NP (Mosley and Hunter, 2003; Baalousha et al., 2008) and multiwalled carbon nanotubes (Hyung et al., 2007) resulting in changes in their physico-chemical proper-

* Corresponding author. Tel.: +44 121 4158133; fax: +44 121 4145528.
E-mail address: a.baker.2@bham.ac.uk (A. Baker).

0045-6535/$ - see front matter © 2009 Elsevier Ltd. All rights reserved.
doi:10.1016/j.chemosphere.2009.04.067

Author's personal copy

ties of the NPs. These interactions are complex, resulting in increased size or decreased dispersion of the NPs, depending on conditions, with dispersion caused by charge and steric stabilisation and aggregation by bridging mechanisms (Klaine et al., 2008).

Fluorescence spectrometry is a technique which permits rapid analysis with widespread applications in water science, including the analysis of HS (Hudson et al., 2007). Fluorescence quenching of dissolved phase HS due to metal complexation has previously been used to study metal–HS interactions (Saar and Weber, 1980; Cabaniss, 1992; Cook and Langford, 1995; Sharpless and McGown, 1999; Cheng and Chi, 2002; Zhao and Nelson, 2005). However, no similar work on metal quenching has been performed on NP–HS interactions. This paper examines the interactions iron oxide NPs and Suwannee River Fulvic acid (SRFA, a well characterised, reference material), based on the fluorescence quenching of FA by the NPs. A fulvic rather than humic acid was used because of greater relevance to aquatic systems.

2. Materials and methods

2.1. Materials

Commercially available chemicals and solvents were purchased from Aldrich and Fisher Scientific. Ultra high purity water with a maximum resistivity of 18 MΩ cm^{-1} was used throughout the experiments. Iron oxide NPs were prepared by the forced hydrolysis of $FeCl_3$ solution (filtered at 200 nm) by addition to a boiling HCl solution (also filtered at 200 nm) and continuing to boil for 10 min (Schwertman and Cornel, 1991; Kendall and Kosseva, 2006). The final suspension of iron oxide NPs had a 1% concentration and was kept at pH 2 from originally added HCl. The total iron concentrations used in quenching experiments was in all cases <1.2 mM. SRFA was purchased from the International Humic Substances Society (IHSS) and used without further modification at 10 mg L^{-1} in all experiments. The mixed suspensions of iron nanoparticles and SRFA were allowed to equilibrate at room temperature for 1 h, and then the pH was altered by adding dilute NaOH to obtain pH values from 2 to 10 and a constant ionic strength of 10^{-3} M in $NaNO_3$. Due to high dissolved iron concentration at low pH, ionic strengths were somewhat higher (<10% change in all cases) at very low pH values (pH < 3). The pH values were checked after 24 h and changed as necessary to appropriate values for experiments with further re-equilibration, until a stable pH was reached. Analysis of pH was performed with a pHM240 electrode from Radiometer analytical. Fluorescence spectra were acquired immediately after pH change (data not shown) and after reaching a stable pH value (generally approximately 24 h).

2.2. Methods

Dynamic light scattering (DLS) measurements (Baalousha et al., 2008) were performed at 20 °C using a Malvern High Performance Particle Sizer (HPPS 5001). The zeta average was obtained as the average of three measurements performed on each sample after 24 h of equilibration. Actual values in such polydisperse samples (especially at high pH) may not be accurate, but DLS measurements give useful information about aggregation status.

Fluorescence intensity was measured using a Varian Cary Eclipse spectrophotometer, equipped with a Peltier temperature controller. Emission scans were performed from 280 to 500 nm, with excitation wavelengths from 200 to 400 nm, both at 5 nm intervals. Uncorrected spectra were combined to form an excitation–emission matrix (EEM). Bandpass was 5 nm, temperature 20 °C and photomultiplier tube voltage set to 725 V. Manufacturer supplied excitation and emission filters were employed to eliminate any light scattered by the NPs from reaching the photomultiplier. Spectrophotometer output was monitored by regular measurement of the Raman intensity of ultra pure water in a sealed cuvette at 348 nm excitation and 5 nm bandpass. Over the analytical period, mean intensity was 23.0 ± 1.1 units.

The theory of quenching fluorescence has been described in detail elsewhere (Lakowicz, 1999; Geddes, 2001). Fluorescence quenching is a process which decreases the intensity of the fluorescence emission. Quenching may occur by a wide range of mechanisms as either static (e.g. equilibrium complexation) or dynamic (e.g. collisional) quenching. Dynamic quenching is a process where the fluorophore and the quencher come into contact during the lifetime of the excited state and involves energy transfer, while static quenching is a process where non-fluorescent complexes of the ground state fluorophore are formed. For monodisperse systems, fluorescence quenching data have a linear dependence when presented as a Stern–Volmer plot i.e. by plotting I_0/I (fluorescence intensity in the absence of quencher/fluorescence intensity in the presence of quencher) against concentration of quencher and deviations from linearity carry information on the nature of the quenching process and fluorophore–quencher interaction. If there is more than one quenching process operating over a range of concentrations or environmental conditions, the Stern–Volmer plots would be non-linear. Therefore exploring the linearity of Stern–Volmer plots is an excellent tool to understand organic matter interactions with iron NPs.

3. Results and discussion

3.1. Aggregation behaviour

Previously we have shown that, when fully disaggregated (at low pH), this iron oxide is 7 ± 3 nm based on a number size distribution from measurements and calculations using atomic force microscopy (AFM), transmission electron microscopy (TEM) and field flow fractionation (FFF) data (Baalousha et al., 2008). In the same study, we also considered aggregation in this system and showed it to be essentially charge dependent, in line with expectations from DLVO theory. Dynamic light scattering (DLS) data for NPs in the absence of SRFA (Fig. 1) agrees with previous work and shows that the NPs aggregate strongly as a function of pH and charge (Baalousha et al., 2008), with maximum aggregation at pH 8. Fig. 1 also shows the detailed aggregation behaviour as a function of SRFA and NP concentration. Larger sizes seen at low pH (where the iron oxide is strongly positively charged) is due to aggregation of the HS, either alone or with the iron oxide NPs. Aggregation is at a maximum at pH 4 when the equimolar ratios

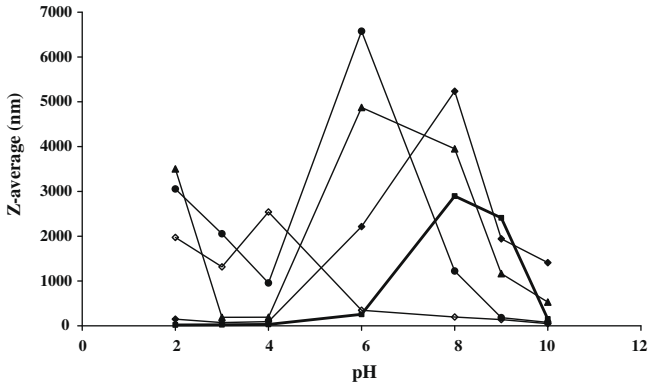

Fig. 1. Dynamic light scattering at different pHs of SRFA with different concentrations of iron NMs (11×10^{-5} M iron NMs (◇), 0.22×10^{-3} M iron NMs (●), 0.56×10^{-3} M iron NMs (▲), 1.12×10^{-3} M iron NMs (♦)) and 1.12×10^{-3} M iron NMs alone (■).

Author's personal copy

of FA:NPs are used, at pH 6 when the equivalent molar ratios (assuming the molar mass of SRFA is 1000 (Lead et al., 2000)) of FA:NPs is 1:22, at pH 7 is 1:56 and at pH 8 is 1:112 electrophoretic mobility data (not shown) indicates good agreement between charge and aggregation, with points of zero charge (pzc) essentially identical to the pH value at which maximum aggregation occurs. This behaviour can be explained by the formation of surface films of HS on the iron oxide NPs (Baalousha et al., 2008). At high HS:Fe ratios, surface coverage is complete and aggregation is shifted to lower pH values, where the HS is less charged (the pzc for HS is approximately pH 2, while for iron oxides is approximately pH 8). As Fe increases (HS:Fe ratio decreases), surface coverage decreases most likely giving a patchy coating where increasing amounts of iron oxide are exposed to solution. The aggregation maximum is then shifted towards higher pH values. At the highest iron oxide concentration, aggregation occurs at the same pH as without any HS, indicating that surface coverage is minimal. Interestingly, aggregation appears to be higher with HS present, despite the charge, perhaps indicating that the HS is bridging iron oxide aggregates forming even larger aggregates.

Ultrafiltration data for this batch of iron oxides (Baalousha et al., 2008) indicates that at pH 2, 35% of the total iron is dissolved i.e. <1 nm, while at pH 3, this value is 10%, pH 4 is at 1% and at higher pH values the dissolved iron concentration is negligible. The iron concentrations used are shown in Fig. 3. For all conditions measured, we therefore have a good understanding of the distribution between dissolved, nanoparticles and aggregated forms of iron, including knowledge of aggregate size.

3.2. Fluorescence and fluorescence quenching

Fluorescence peaks associated with fulvic substances (fulvic-like fluorescence), for fresh water samples are observed at 300–340 nm excitation and 400–460 nm emission (see review by Hudson et al., 2007). The representative EEM spectra at 20 °C for pH 3 and 8 for fulvic acid with and without 0.22×10^{-3} M iron nanoparticles are shown in Fig. 2. Fig. 3 presents Stern–Volmer plots associated with addition of different concentrations of Fe nanoparticles at pH values examined, from pH 2 to pH 10. Given the distribution between aggregates, dispersed particles and dissolved phase species discussed above, quenching of fluorescence intensity at all pH clearly shows that all forms of iron (dissolved and dispersed and aggregated NPs) interact with SRFA and quench fluorescence. From the literature, we expect the dissolved form to quench HS fluorescence (Cheng and Chi, 2002; Zhao and Nelson, 2005), but this is the first data showing NP quenching.

Fig. 3 shows that the Stern–Volmer plots are non-linear and this indicates a complex quenching behaviour between the iron species including the dispersed nanoparticles and their aggregates and the SRFA. This quenching most likely involves both static and dynamic quenching mechanisms. Zhao and Nelson (2005) in a fluorescence quenching study of SRFA in the presence of dissolved Fe(III) at pH 4 demonstrated that both dynamic and static quenching were involved. The non-linear Stern–Volmer plots can be caused by the presence of polydisperse and complex fluorophores and quenchers; it is well known that HS is highly heterogeneous and polydisperse (Lead and Wilkinson, 2006) and our data here have shown that these iron oxide NPs are equally complex. At pH 2 and 3 the Stern–Volmer plots are the most linear and have the lowest rate of quenching with iron concentration; at these pH values most of the iron is present as dispersed nanoparticles, with a substantial proportion present as the dissolved phase.

Maximum quenching coincides with the maximum aggregation (maximum values of aggregate size) which occur at pH values of 6–8 (Fig. 1; Baalousha et al., 2008). Aggregates appear to be more efficient quenchers than either dissolved Fe or Fe oxide NPs.

The Stern–Volmer plots at both pH 9 and 10 (Fig. 3) show an interesting trend, with a decrease in the I_0/I ratio at the highest iron oxide concentrations, just where DLS data indicates that disaggregation begins to occur, most likely due to increased negative

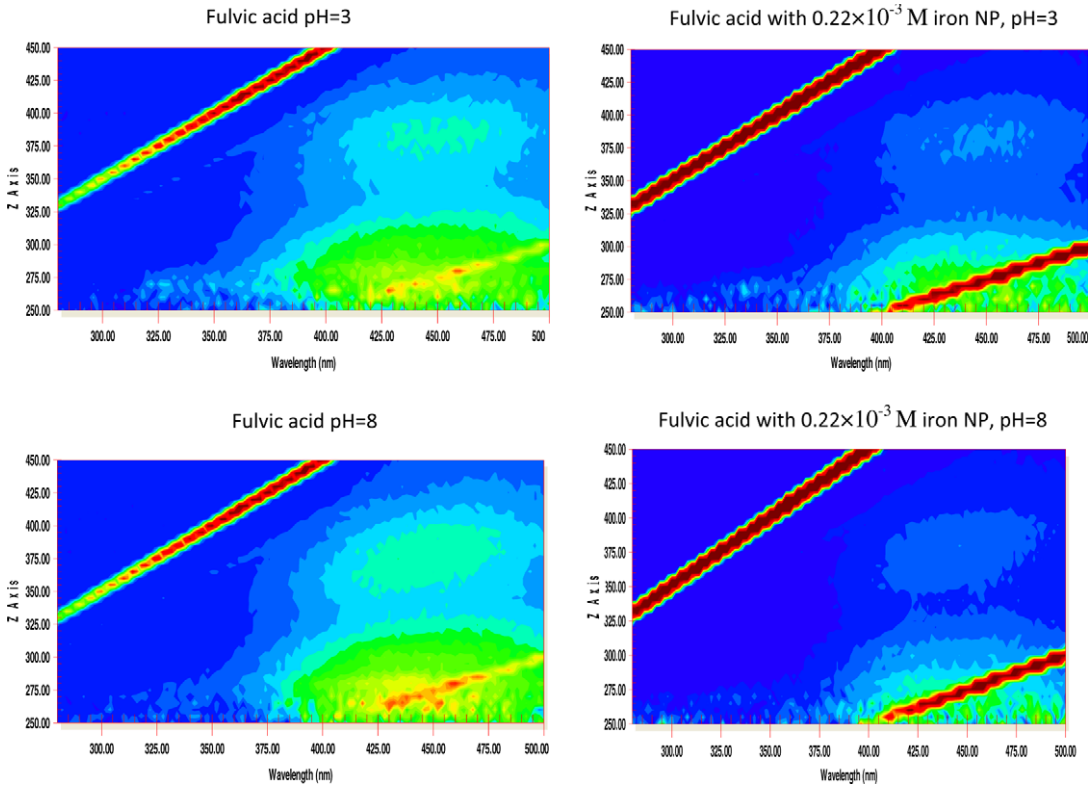

Fig. 2. Fluorescence EEMs at 20 °C of SRFA with (right) and without (left) iron nanoparticles (0.22×10^{-3} M) and pH 3 (top) and pH 8 (bottom).

Author's personal copy

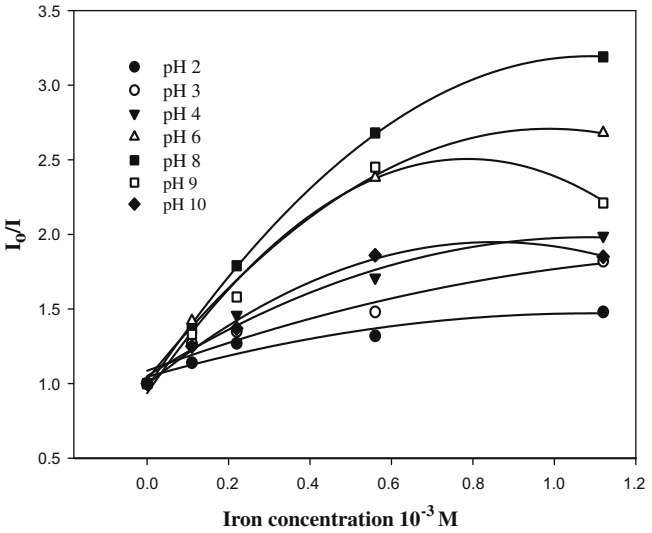

Fig. 3. Quenching of fulvic acid fluorescence intensity by iron nanoparticles at different pH (2–10).

charges at high pH (data not shown). No other pH values show this behaviour. The observed trend could be related to pH based conformational or chemical changes (leading to electronic changes) in the SRFA, e.g. full deprotonation of carboxylic and other functional groups leading to charge repulsion and change in the conformation of the SRFA as pH increases. However, as this only occurs at the highest pH where charging of the HS is already near maximal makes this unlikely. The most likely explanation for the trend is related to the disaggregation of the iron oxides at pH 9 and 10 (Fig. 1), again indicating that the NP aggregates are the most powerful quenchers compared with the dissolved or primary particle.

4. Conclusions

Iron oxide NPs were synthesised and their pH- and concentration-dependent aggregation was observed, with aggregation highest at pH 7–8, which coincides with the point of zero charge (Baalousha et al., 2008). This conclusion is also in line with our previous work. Quenching due to iron NPs was non-linear, indicative of polydisperse and complex materials, with quenching probably due to both static and dynamic mechanisms occurring. Greater quenching at higher nanoparticle concentration indicated changes in NP:SRFA interactions with NP concentration. The effect of concentration is masked partly as the different phases (dissolved, nanoparticulate and aggregated) quench the SRFA fluorescence to different extents. In addition, fluorescence quenching at a constant NP concentration (and SRFA ratio) is highly pH dependent, strongly reflecting the form of NP (dissolved, dispersed NP or aggregated NP). The aggregated form of iron was found to be the strongest quencher, assuming no chemical reactions occurred.

In conclusion, fluorescence quenching is a simple, powerful and effective probe for determining the nature of interactions between inorganic nanoparticles and natural organic macromolecules. This first application of the method shows its potential and the necessity of combining the techniques with others such as DLS to provide a full description of the test system.

Acknowledgements

This work was funded by the European Union Framework programm VI Marie Curie Early stage Training scheme (MEST-CT-2004-504356).

References

Aiken, G.R., McKnight, D.M., Wershaw, R.L., MacCarthy, P., 1985. Humic Substances in Soil, Sediment, and Water: Geochemistry, Isolation and Characterization. John Wiley and Sons, New York.

Baalousha, M., Manciulea, A., Cumberland, S., Lead, J.R., Kendal, K., 2008. Aggregation and surface properties of iron oxide nanoparticles: influence of ph and natural organic matter. Environ. Toxicol. Chem. 27, 1875–1882.

Bermudez, E., Mangum, J.B., Wong, B.A., Asgharian, B., Hext, P.M., Warheit, D.B., Everitt, J.I., 2004. Pulmonary responses of mice, rats, and hamsters to subchronic inhalation of ultrafine titanium dioxide particles. Toxicol. Sci. 77, 347–357.

Brayner, R., Ferrari-Iliou, R., Brivois, N., Djediat, S., Benedetti, M.F., Fievet, F., 2006. Toxicological impact studies based on Escherichia coli bacteria in ultrafine ZnO nanoparticles colloidal medium. Nano Lett. 6, 866–870.

Buffle, J., 2006. The key role of environmental colloids/nanoparticles for the sustainability of life. Environ. Chem. 3, 155–158.

Cabaniss, S.E., 1992. Synchronous fluorescence spectra of metal-fulvic acid complexes. Environ. Sci. Technol. 6, 1133–1139.

Casey, A., Davoren, M., Herzog, E., Lyng, F.M., Byrne, H.J., Chambers, G., 2007. Probing the interaction of single walled carbon nanotubes within cell culture medium as a precursor to toxicity testing. Carbon 45, 34–40.

Chen, K.L., Elimelech, M., 2007. Influence of humic acid on the aggregation kinetics of fullerene (C60) nanoparticles in monovalent and divalent electrolyte solutions. J. Colloids Interf. Sci. 309, 126–134.

Chen, J., LeBoeuf, E.J., Dai, S., Gu, B., 2003. Fluorescence spectroscopic studies of natural organic matter fractions. Chemosphere 50, 639–647.

Cheng, W.P., Chi, F.H., 2002. A study of polyferric sulfate reacting with humic acid using a fluorescence-quenching method. Water. Res. 36, 4583–4591.

Cook, R.L., Langford, C.H., 1995. Metal ion quenching of fulvic acid fluorescence intensities and lifetimes: nonlinearities and a possible three-component model. Anal. Chem. 67, 174–180.

Diegoli, S., Manciulea, A.L., Begum, S., Jones, I.P., Lead, J.R., Preece, J.A., 2008. Interaction between manufactured gold nanoparticles and naturally occurring organic macromolecules. Sci. Total Environ. 402, 51–61.

Fabregas, J., Renshaw, J., Lead, J.R., in press. Silver nanoparticle impact on bacterial growth: effect of pH, concentration and organic matter. Environ. Sci. Technol.

Fortner, J.D., Lyon, D.Y., Sayes, C.M., Boyd, A.M., Falkner, J.C., Hotze, E.M., Alemany, L.B., Tao, Y.J., Guo, W., Ausman, K.D., Colvin, V.L., Hughes, J.B., 2005. C60 in water: nanocrystal formation and microbial response. Environ. Sci. Technol. 39, 4307–4316.

Geddes, C.D., 2001. Optical halide sensing using fluorescence quenching: theory, simulations and applications – a review. Meas. Sci. Technol. 12, R53–R88.

Giasuddin, A.B.M., Kanel, S.R., Choi, H., 2007. Adsorption of humic acid onto nanoscale aerovalent iron and its effect on arsenic removal. Environ. Sci. Technol. 41, 2022–2027.

Hu, S., Cook, S., Weng, P., Hwang, H.-M., 2009. In vitro evaluation of cytotoxicity of engineered metal oxide nanoparticles. Sci. Total Environ. 407, 3070–3072.

Hudson, N., Baker, A., Reynolds, D., 2007. Fluorescence analysis of dissolved organic matter in natural, waste and polluted waters – a review. River Res. Appl. 23, 631–649.

Hyung, H., Fortner, J.D., Hughes, J.B., Kim, J.-H., 2007. Natural organic matter stabilizes carbon nanotubes in the aqueous phase. Environ. Sci. Technol. 41, 179–184.

Jia, G., Wang, H., Yan, L., Wang, X., Pei, R., Yan, T., Zhao, Y., Guo, X., 2005. Cytotoxicity of carbon nanomaterials: single-wall nanotube, multi-wallnanotube, and fullerene. Environ. Sci. Technol. 39, 1378–1383.

Kendall, K., Kosseva, M.R., 2006. Nanoparticle aggregation influenced by magnetic fields. Colloids Surf. A 286, 112–116.

Klaine, S.J., Alvarez, P.J.J., Batley, G.E., Fernandes, T.F., Handy, R.D., Lyon, D., Mahendra, S., McLaughlin, M.J., Lead, J.R., 2008. Nanomaterials in the environment: fate, behaviour, bioavailability and effects. Environ. Toxicol. Chem. 27, 1825–1851.

Lacerda, L., Bianco, A., Prato, M., Kostarelos, K., 2006. Carbon nanotubes as nanomedicines: from toxicology to pharmacology. Adv. Drug Deliver. Rev. 58, 1460–1470.

Lakowicz, J.R., 1999. Principles of Fluorescence Spectroscopy, second ed. Plenum Press, New York.

Lead, J.R., Wilkinson, K.J., 2006. Natural aquatic colloids: current knowledge and future trends. Environ. Chem. 3, 159–171.

Lead, J.R., Wilkinson, K.J., Starchev, K., Canonica, S., Buffle, J., 2000. Determination of diffusion coefficients of humic substances by fluorescence correlation spectroscopy: role of solution conditions. Environ. Sci. Technol. 34, 1365–1369.

Lyon, D.Y., Adams, L.K., Faulkner, J.C., Alvarez, P.J.J., 2006. Antibacterial activity of fullerene water suspensions: effect of preparation method and particle size. Environ. Sci. Technol. 40, 4360–4366.

Lyven, B., Hassellhov, M., Turner, D.R., Haraldsson, C., Andersson, K., 2003. Competition between iron- and carbon-based colloidal carriers of trace metals in a freshwater assessed using flow field-flow fractionation coupled to ICPMS. Geochim. Cosmochim. Acta 67, 3791–3802.

Madden, A.S., Hochella, M.F., 2005. A test of geochemical reactivity as a function of mineral size: manganese oxidation promoted by haematite nanoparticles. Geochim. Cosmochim. Acta 69, 389–398.

Madden, A.S., Hochella, M.F., Luxton, T.P., 2006. Insights for size-dependent reactivity of haematite nanomineral surfaces through Cu^{2+} sorption. Geochim. Cosmochim. Acta 70, 4095–4104.

Author's personal copy

Mosley, L.M., Hunter, K.A., 2003. Forces between colloid particles in natural waters. Environ. Sci. Technol. 37, 3303–3308.
Muller, J., Huaux, F., Lison, D., 2006. Respiratory toxicity of carbon nanotubes: how worried should we be? Carbon 44, 1048–1056.
Nowack, B., Bucheli, T.D., 2007. Occurrence, behavior and effects of nanoparticles in the environment. Environ. Pollut. 150, 5–22.
Nurmi, J.T., Tratnyek, P.G., Sarathy, V., Baer, D.R., Amonette, J.E., Pecher, K., Wank, C., Linehan, J.C., Matson, D.W., Penn, R.L., Driessen, M.D., 2005. Characterization and properties of metallic iron nanoparticles: spectroscopy, electrochemistry, and kinetics. Environ. Sci. Technol. 39, 1221–1230.
Oberdorster, E., 2004. Manufactured nanomaterials (Fullerenes, C60) induce oxidative stress in the brain of juvenile largemouth bass. Environ. Health Perspect. 112, 1058–1062.
Oyewumi, M.O., Yokel, R.A., Jay, M., Coakley, T., Mumper, R.J., 2004. Comparison of cell uptake, biodistribution and tumor retention of folate-coated and PEG-coated gadolinium nanoparticles in tumor-bearing mice. J. Control. Release 95, 613–626.
Paradise, M., Goswami, T., 2007. Carbon nanotubes – production and industrial applications. Mater. Design 28, 1477–1489.
Phenrat, T., Saleh, N., Sirk, K., Tilton, R.D., Lowry, G.V., 2007. Aggregation and sedimentation of aqueous nanoscale zerovalent iron dispersions. Environ. Sci. Technol. 41, 284–290.
Ponder, S.M., Darab, J.G., Bucher, J., Caulder, D., Craig, I., Davis, L., Edelstein, N., Nitsche, H., Rao, L., Shuh, D.K., Mallouk, T.E., 2001. Surface chemistry and electrochemistry of supported zerovalent iron nanoparticles in the remediation of aqueous metal contaminants. Chem. Mater. 13, 479–486.
Saar, R.A., Weber, J.H., 1980. Comparison of spectrofluorometry and ion-selective electrode potentiometry for determination of complexes between fulvic acid and heavy metal ions. Anal. Chem. 52, 2095–2100.
Schwertman, U., Cornel, R.M., 1991. Iron Oxides in the Laboratory. Whiley VCH, Weinheim.
Seeger, E.M., Baun, A., Kasstner, M., Trapp, S., 2009. Insignificant acute toxicity of TiO_2 nanoparticles to willow trees. J. Soils Sedim. 9, 46–53.
Sharpless, C., McGown, L.B., 1999. Effects of aluminum-induced aggregation on the fluorescence of humic substances. Environ. Sci. Technol. 33, 3264–3270.
Smith, C.J., Shaw, B.J., Handy, R.D., 2007. Toxicity of single walled carbon nanotubes to rainbow trout, (*Oncorhynchus mykiss*): respiratory toxicity, organ pathologies, and other physiological effects. Aquat. Toxicol. 82, 94–109.
Soto, K.F., Carrasco, A., Powell, T.G., Garza, K.M., Murr, L.E., 2005. Comparative in vitro cytotoxicity assessment of some manufactured nanoparticulate materials characterized by transmission electron microscopy. J. Nanopart. Res. 7, 145–169.
Tian, F., Cui, D., Schwarz, H., Estrada, G.G., Kobayashi, H., 2006. Cytotoxicity of single-wall carbon nanotubes on human fibroblasts. Toxicol. In Vitro 20, 1202–1212.
Wiesner, M.R., Lowry, G.V., Alvarez, P., Dionysiou, D., Biswas, P., 2006. Assessing the risks of manufactured nanomaterials. Environ. Sci. Technol. 40, 4336–4345.
Zhang, W.S., 2003. Nanoscale iron particles for environmental remediation: an overview. J. Nanopart. Res. 5, 323–332.
Zhao, J., Nelson, D., 2005. Fluorescence study of the interaction of Suwannee River fulvic acid with metal ions and Al^{3+}–metal ion competition. J. Inorg. Biochem. 99, 383–396.